Highly Efficient Relativistic-Ion Generation in the Laser-Piston Regime

T. Esirkepov,[1,*] M. Borghesi,[2] S.V. Bulanov,[1,2,†] G. Mourou,[3] and T. Tajima[1]
[1]*Kansai Research Establishment, JAERI, Umemidai 8-1 Kizu, Kyoto 619-0215, Japan*
[2]*The Queen's University of Belfast, Belfast BT7 1NN, United Kingdom*
[3]*Center for Ultrafast Optical Science, University of Michigan, Ann Arbor, Michigan 48109, USA*
(Received 10 December 2003; published 27 April 2004)

An intense laser-plasma interaction regime of the generation of high density ultrashort relativistic ion beams is suggested. When the radiation pressure is dominant, the laser energy is transformed efficiently into the energy of fast ions.

DOI: 10.1103/PhysRevLett.92.175003 PACS numbers: 52.38.Kd, 29.25.–t, 41.75.Lx, 52.65.Rr

Today the laser drive of *relativistic* ions is an attractive goal of the intense laser-matter interaction physics. Direct laser acceleration of protons to relativistic energies requires intensity $I_p = 4.6 \times 10^{24}$ W/cm$^2 \times (1\ \mu\text{m}/\lambda)^2$, corresponding to the dimensionless amplitude $a \equiv eE/m_e\omega c = m_p/m_e \approx 1836$, where E, λ, and ω are the electric field, wavelength, and frequency of the electromagnetic (EM) wave, e and m_e are the electron charge and mass, and m_p is the proton mass. In a plasma, because of collective effects, protons can gain relativistic energies at much less intensity, about 10^{21} W/cm$^2 \times (1\ \mu\text{m}/\lambda)^2$, as is exemplified in the theory of the strongly nonlinear hybrid electron-ion wakefield induced by a short EM wave packet with the dimensionless amplitude a greater than $(m_p/m_e)^{1/2} \approx 43$ and the Coulomb explosion of an overdense plasma region with the size of a few microns when a relativistically strong EM wave sweeps all the electrons away [1]. In general, the laser-driven ion acceleration arises from charge separation caused by the EM wave. Various regimes have been discussed in the framework of this concept: the plasma thermal expansion into vacuum [2], the Coulomb explosion of a strongly ionized cluster [3], transverse explosion of a self-focusing channel [4], and ion acceleration in the strong charge separation field caused by a quasistatic magnetic field [5].

In this Letter we present the regime of the high density ultrashort relativistic ion beam generation from a thin foil by an ultraintense EM wave. We call this regime the "laser piston" (LP). In contrast to previously discussed schemes, in this regime the ion beam generation is highly efficient and the ion energy per nucleon is proportional to the laser pulse energy. Our analytical estimation conforms to the result of three-dimensional (3D) particle-in-cell (PIC) simulations. In comparison with the experimental experience of present-day petawatt lasers, the LP regime predicts yet another advantage of the exawatt lasers, in addition to possible applications depicted in [6].

We distinguish the following two stages of the LP operation. (i) A relativistically strong laser pulse irradiates a thin foil with thickness l and electron density n_e. The laser pulse waist is sufficiently wide, so the quasi-one-dimensional geometry is in effect. Electrons are quickly accelerated up to $v_e \sim c$ by the transverse electric field, E_L, of the laser pulse, and they are pushed in the forward (longitudinal) direction by the force $|e\mathbf{v}_e \times \mathbf{B}_L/c| \approx eE_L$, where B_L is the magnetic field of the laser pulse. Assume that all the electrons are displaced in the longitudinal direction, then the charge separation field, $E_\parallel = 2\pi e n_e l < E_L$, between the electron and ion layers does not depend on the separation distance. In this longitudinal field the ion energy $\mathcal{E}_i = [m_i^2c^4 + (eE_\parallel ct)^2]^{1/2}$ becomes relativistic in a time of the order of $t_{ri} = (m_i c/eE_\parallel)$. We find that the ion layer can be accelerated up to relativistic energies during N_L laser cycles under the condition $E_L > 2\pi e n_e l \gtrsim m_i\omega c/2\pi e N_L$. Hence, to produce relativistic protons in one laser cycle we need an EM wave with $E_L > 300 m_e\omega c/e$, $I_L > 1.2 \times 10^{23}$ W/cm$^2 \times (1\ \mu\text{m}/\lambda)^2$, and the pulse waist must be much greater than $ct_{ri} \simeq \lambda$. (ii) The accelerated foil, which consists of the electron and ion layers, can be regarded as a relativistic plasma mirror copropagating with the laser pulse. Assume that the laser pulse is perfectly reflected from this mirror. In the laboratory reference frame, before the reflection it has the energy $\mathcal{E}_L \propto E_L^2 L$, and after the reflection its energy becomes much lower: $\tilde{\mathcal{E}}_L \propto \tilde{E}_L^2 \tilde{L} \approx E_L^2 L/4\gamma^2$. Here the incidence laser pulse length is equal to L, the reflected pulse length $\tilde{L}$ is longer by a factor of $4\gamma^2$, and the transverse electric field is smaller by a factor of $4\gamma^2$, where $\gamma = (1 - v^2/c^2)^{-1/2}$ is the Lorentz factor of the plasma mirror. Hence, the plasma mirror acquires the energy $(1 - 1/4\gamma^2)\mathcal{E}_L$ from the laser pulse. At this stage the plasma (the electrons and, hence, ions) is accelerated due to the radiation pressure. The radiation momentum is transferred to ions through the charge separation field, and the "longitudinal" kinetic energy of ions is much greater than that of electrons. We note that the specified intensity is close to the limit where individual electrons undergo a substantial radiation friction effect [7]. However, when the foil is accelerated up to relativistic energy, this effect becomes weaker because its strength measure, $4\pi r_e/3a^3\lambda$, is reduced by 2γ in the foil reference frame ($r_e = e^2/m_e c^2$ is the classical electron radius).

We notice a connection of the plasma layer acceleration scheme, presented above, with a mechanism of the ion acceleration proposed by Veksler [8], as well as with the "snow plow" acceleration mechanism revealed in

Ref. [9]. Formulated in the mid-1950s Veksler's concept of the collective acceleration of ions in an electron-ion bunch moving in a strong electromagnetic wave had a great influence upon both particle accelerator technology and plasma physics. Up to now its direct realization was considered at moderate driving EM radiation intensities, when transverse instabilities impede the acceleration [10]. As we show below using 3D PIC simulations, in our scheme the transverse instabilities are suppressed or retarded due to the following. (i) The plasma layers become relativistic quickly, during one or more laser wave periods, in the first stage of the acceleration. Because of relativistic effects the transverse instabilities grow in the laboratory frame γ times slower than in the plasma reference frame. (ii) The radiation pressure causes a stretching of the plasma mirror in the transverse direction, so the transverse instabilities can be retarded similarly to the slowing down of the Jeans instability in the theory of the expanding early universe [11].

In order to examine the present scheme in three-dimensional geometry, whose effects may play a crucial role in the dynamics and stability of the plasma layer under the action of a relativistically strong laser pulse, we carried out 3D PIC simulations with the code REMP based on the "density decomposition" scheme [12]. In the simulations the laser pulse is linearly polarized along the z axis; it propagates along the x axis. Its dimensionless amplitude is $a = 316$ corresponding to the peak intensity $I = 1.37 \times 10^{23}$ W/cm$^2 \times (1\ \mu\text{m}/\lambda)^2$. The laser pulse is almost Gaussian with FWHM size $8\lambda \times 25\lambda \times 25\lambda$, it has a sharp front starting from $a = 100$, its energy is $\mathcal{E}_L = 10$ kJ $\times (\lambda/1\ \mu\text{m})$. The target is a 1λ thick plasma slab with density $n_e = 5.5 \times 10^{22}$ cm$^{-3} \times (1\ \mu\text{m}/\lambda)^2$, which corresponds to the Langmuir frequency $\omega_{pe} = 7\omega$. For $\lambda \simeq 1\ \mu$m the laser pulse electric field is strong enough to strip even high-Z atoms in much shorter time than the laser wave period; thus, we assume that the plasma is fully ionized. The ions and electrons have the same absolute charge, and their mass ratio is $m_i/m_e = 1836$. The simulation box size is $100\lambda \times 72\lambda \times 72\lambda$ corresponding to the grid size $2500 \times 1800 \times 1800$, so the mesh size is 0.04λ. The total number of quasiparticles is 4.37×10^9. The boundary conditions are periodic along the y and z axes and absorbing along the x axis for both the EM radiation and the quasiparticles. Simulation results are shown in Figs. 1–3, where the space and time units are the laser wavelength λ and period $2\pi/\omega$.

Figure 1 shows the ion density and x component of the EM energy flux density (the Poynting vector). We see that the region of the foil corresponding to the size of the laser focal spot is pushed forward. Although the plasma in the foil is overcritical, it is initially *transparent* for the laser pulse due to the effect of relativistic transparency (see, e.g., Ref. [13]). Therefore a portion of the laser pulse passes through the foil. Eventually it accelerates electrons and, as a result of the charge separation, a longitudinal electric field is induced. This can be interpreted as a rectification of the laser light, by the analogy with a rectifier in electrical engineering: the transverse oscillating electric field is transformed into a longitudinal quasistatic electric field. The dimensionless amplitude of the longitudinal field is $a_\parallel \approx 150$ corresponding to $E_\parallel = 4.8 \times 10^{14}$ V/m $\times (1\ \mu\text{m}/\lambda)$. The typical distance of the charge separation is comparable with the initial thickness of the foil and is much less than the transverse size of the region being pushed. The ion layer is accelerated by this longitudinal field. This stage corresponds to the first step of the LP scheme. As the foil moves more and more rapidly, in its proper frame the incident wavelength increases; thus, the accelerating foil becomes less transparent with time.

As seen in the cross section of the Poynting vector in Fig. 1(a), the thickness of the red stripes, corresponding to half of the radiation wave length, increases from left to right (along the x axis). The increase is weaker at the

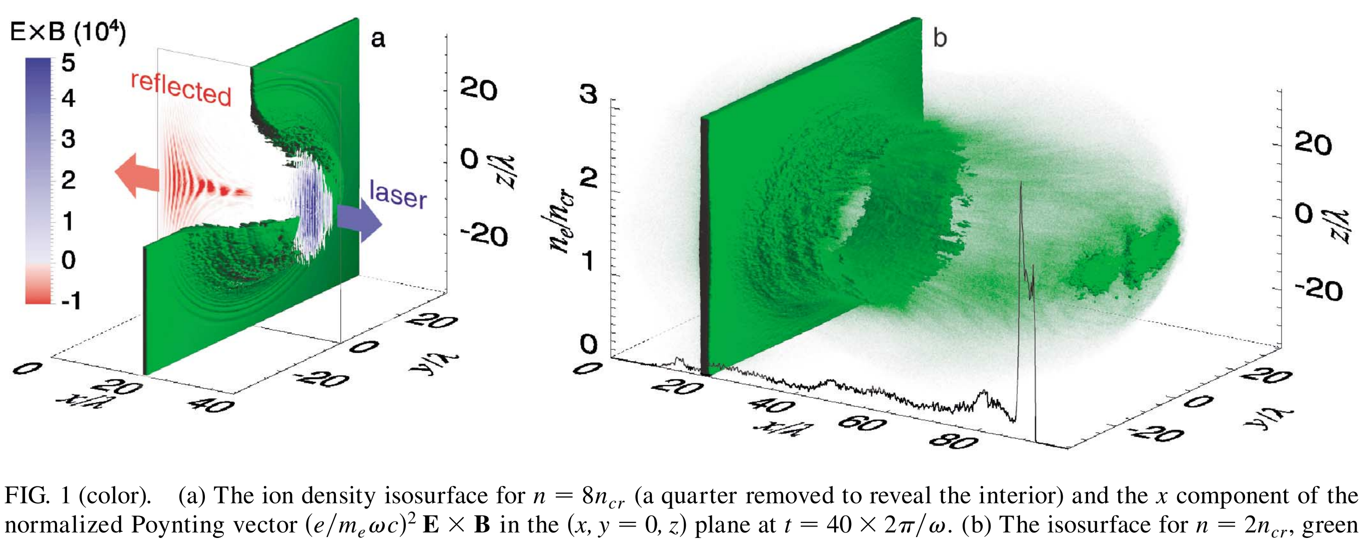

FIG. 1 (color). (a) The ion density isosurface for $n = 8n_{cr}$ (a quarter removed to reveal the interior) and the x component of the normalized Poynting vector $(e/m_e\omega c)^2\, \mathbf{E} \times \mathbf{B}$ in the $(x, y = 0, z)$ plane at $t = 40 \times 2\pi/\omega$. (b) The isosurface for $n = 2n_{cr}$, green gas for lower density at $t = 100 \times 2\pi/\omega$; the black curve shows the ion density along the laser pulse axis.

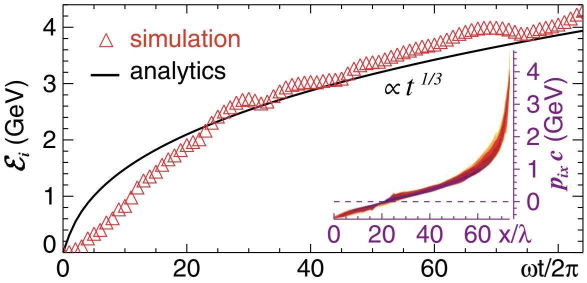

FIG. 2 (color). The maximum ion kinetic energy versus time and the ion phase space projection (x, p_x) at $t = 80 \times 2\pi/\omega$.

periphery (in the transverse direction); correspondingly, we see distinctive phase curves. This "anisotropic redshift" results from the relativistic Doppler effect when the laser pulse is reflected from the copropagating accelerating and deforming relativistic mirror. The redshift testifies that the laser pulse is expending its energy for the acceleration of the plasma mirror, as specified above in the second stage of the LP scenario. The foil is transformed into a "cocoon" where the laser pulse is almost confined. The accelerated ions form a nearly flat thin *plate* with high density, Fig. 1(b).

Figure 2 shows the ion maximum energy versus time and the ion phase space plot. The dependence is initially linear; at later times it scales as $t^{1/3}$. The ion and electron energy spectra and transverse emittances are presented in Fig. 3. The number of ions in the plate is $\mathcal{N}_i = 2 \times 10^{12}$, their energies are from 1.4 to 3.2 GeV. The efficiency of the energy transformation from laser to ions is greater than 40%. The ion bunch density is 3×10^{21} cm^{-3}, its duration is 20 fs, its transverse emittance is less than 0.1π mm mrad. As the plate is quasineutral, the average longitudinal velocity of the electron bulk is about that of ions, $v_{e\parallel} \approx v_{i\parallel}$; thus, the average longitudinal energy of electrons is of the order of $\mathcal{E}_{e\parallel} \simeq (m_e/m_i)\mathcal{E}_i$. Correspondingly, the energy spectrum of electrons is peaked at much less energy than that of ions, Fig. 4.

According to our 2D and 3D simulations at lower intensities, corresponding to petawatt and multipetawatt pulses, the interaction exhibits a continuous transition from regimes of Refs. [1,2,4,5] to the LP regime as the intensity increases.

Here we estimate the ion maximum energy and the acceleration efficiency in the model of the flat foil driven by the EM radiation pressure, as described above in the LP scenario. In general, the radiation pressure on the foil depends on its reflectance [14]. Assume that in the instantaneous reference frame, where the foil is at rest, the relative amplitudes of reflected and transmitted waves are ρ and τ, respectively. Here $|\rho|^2 + |\tau|^2 = 1$ because of energy conservation. The radiation pressure is the sum of the incident, reflected, and transmitted EM wave momentum fluxes, $P = (E_L'^2/4\pi)(1 + |\rho|^2 - |\tau|^2) = (E_L^2/2\pi) \times (\omega'/\omega)^2|\rho(\omega')|^2$. Here the primed values correspond to the moving reference frame, variables without a prime are taken in the laboratory frame. In a quasi-one-dimensional geometry, at the foil location $x(t)$ the laser electric field is $E_L = E_L[t - x(t)/c]$. If the foil is accelerated as a single whole, in its reference frame the incident radiation frequency becomes smaller and smaller with time, thus the reflection becomes more and more efficient and $|\rho(\omega')|^2$ becomes closer to unity. In fact, the foil reference frame is not inertial since the foil is accelerated. Hence, the EM wave frequency ω' decreases with time in this frame as described in Ref. [15]. Nevertheless, we can assume that the acceleration is relatively small and thus $(\omega'/\omega)^2 = (c - v)/(c + v)$, where $v = dx/dt$ is the foil instantaneous velocity.

As is well known, the EM radiation pressure is a relativistic invariant [14]; therefore, we can write the foil motion equation as

$$\frac{dp}{dt} = \frac{E_L^2[t - x(t)/c]}{2\pi n_e l}|\rho(\omega')|^2 \frac{\sqrt{m_i^2c^2 + p^2} - p}{\sqrt{m_i^2c^2 + p^2} + p}, \quad (1)$$

where p is the momentum of ions representing the foil. In the simplest case, when $E_L = \mathrm{const}$ and $|\rho|^2 = 1$, the solution $p(t)$ is an algebraic function of t. For the initial condition $p = p_0$ at $t = 0$ it can be written in a compact form as $p = m_i c[\sinh(u) - \mathrm{csch}(u)/4]$, where $u = (1/3) \times \mathrm{arcsinh}(\Omega t + h_0^3/2 + 3h_0/2)$, $\mathrm{csch}(u) = 1/\sinh(u)$, $\Omega = 3E_L^2/2\pi n_e l m_i c$, and $h_0 = p_0/m_i c + (1 + p_0^2/m_i^2c^2)^{1/2}$.

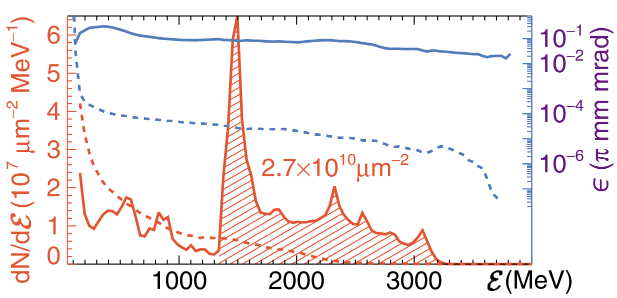

FIG. 3 (color). The energy spectrum (red) and transverse emittance (blue) of ions (solid) and electrons (dashed) located in the box $50\lambda < x < 80\lambda$, $-\lambda < y$, $z < \lambda$ at $t = 80 \times 2\pi/\omega$. The hatched region contains 2.7×10^{10} μm^{-2} particles per cross section. Values correspond to $\lambda = 1$ μm.

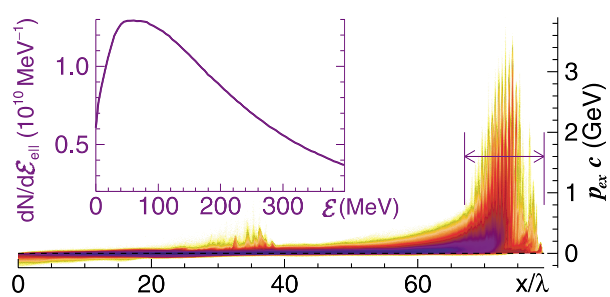

FIG. 4 (color). The electron phase space projection (x, p_x) at $t = 80 \times 2\pi/\omega$ and longitudinal kinetic energy $\mathcal{E}_{e\parallel} = (m_e^2c^4 + p_x^2c^2)^{1/2} - m_ec^2$ spectrum of electrons in the marked interval $67\lambda < x < 80\lambda$.

The ion kinetic energy is $\mathcal{E}_{i\,\mathrm{kin}} = m_i c^2[\sinh(u) + \mathrm{csch}(u)/4 - 1]$. As $t \to \infty$ it asymptotically tends to $\mathcal{E}_{i\,\mathrm{kin}} \approx m_i c^2 (3E_L^2 t/8\pi n_e l m_i c)^{1/3}$. This motion is analogous to that of a charged particle driven by a radiation pressure [14], but in our case the role of the Thomson cross section is played by the quantity $2/n_e l$.

To find an upper limit of the ion energy acquired due to the interaction with a laser pulse of finite duration, we must include the dependence of the laser EM field on space and time. Because of the foil motion, the interaction time can be much longer than the laser pulse duration t_L. Therefore, it is convenient to consider the dynamics in terms of the dimensionless variable

$$\psi = \int_{-\infty}^{t-x(t)/c} \frac{E_L^2(\zeta)}{4\pi n_e l m_i c} d\zeta, \tag{2}$$

which can be interpreted as the normalized energy of the laser pulse portion that has been interacting with the moving foil by time t. Its maximum value is $\max\{\psi\} = \mathcal{E}_L/\mathcal{N}_i m_i c^2$, where $\mathcal{E}_L$ is the laser pulse energy, $\mathcal{N}_i$ is the number of ions in the foil. The solution of Eq. (1), rewritten in terms of ψ, gives the ion kinetic energy

$$\mathcal{E}_{i\,\mathrm{kin}} = m_i c^2 \frac{(2\varkappa\psi + h_0 - 1)^2}{2(2\varkappa\psi + h_0)}, \tag{3}$$

$\varkappa = \frac{1}{\psi}\int_0^{\psi} |\rho(\omega')|^2 d\psi$. The upper limit of the ion kinetic energy and, correspondingly, the laser to ion energy transformation efficiency can be found from Eq. (3) substituting $\psi = \max\{\psi\}$:

$$\max\{\mathcal{E}_{i\,\mathrm{kin}}\} = \frac{2\varkappa\mathcal{E}_L}{2\varkappa\mathcal{E}_L + \mathcal{N}_i m_i c^2} \frac{\varkappa\mathcal{E}_L}{\mathcal{N}_i}, \tag{4}$$

where we set $p_0 = 0$ for simplicity. Here $\varkappa$ is the reflection coefficient, taken in the comoving reference frame, averaged over the foil motion path; $0 < \varkappa \leq 1$. We see that if $\mathcal{E}_L \gg N_i m_i c^2/2$, in this model almost all the energy of the laser pulse is transformed into ion kinetic energy. Using Eq. (4) and the $t^{1/3}$ asymptotic dependence of the ion energy on time, for given simulation parameters we estimate the acceleration time and length as $t_{\mathrm{acc}} \approx (2/3)(\mathcal{E}_L/\mathcal{N}_i m_i c^2)^2 t_L = 16\,\mathrm{ps}$ and $x_{\mathrm{acc}} \approx c t_{\mathrm{acc}} = 4.8\,\mathrm{mm}$, respectively. In the presented simulations the acceleration time is limited by computer resources. However, the analytical estimation Eq. (4) allows us to conclude that at given simulation parameters the limiting ion kinetic energy is 30 GeV. Since the ion bunch is relativistic, another ultraintense laser pulse, sent with proper delay, can accelerate the bunch further.

In conclusion, the LP regime of ultraintense laser-plasma interaction can be employed in a laser-driven heavy ion collider. In the collision of two ion bunches the number of reactions with cross section σ is $\mathcal{N} = \sigma\mathcal{N}_i^2/s$, where s is the bunch sectional area. Adopting the presented simulation parameters, we obtain $\mathcal{N} \approx 2 \times 10^{30}\sigma/\mathrm{cm}^2$. Provided that the energy is high enough so that $\sigma \approx 10^{-24}\ \mathrm{cm}^2$, we can get about a million events in a few femtosecond shot. As suggested by Tajima and Mourou [6], one can get a short multiexawatt laser pulse with sufficient contrast ratio (10^{-12}) using the megajoule NIF facility and present-day technology. Then the resulting ion bunch energy can be over 100 GeV per nucleon, which is suitable for the quark-gluon plasma studies [16]. The laser piston regime, being one of the examples of what we call the relativistic engineering, can give us a promising and unique tool for nuclear physics research.

We thank M. Yamagiwa for significant remarks. We thank H. Daido, J. Koga, K.W. D. Ledingham, P. Migliozzi, K. Nishihara, F. Pegoraro, F. Terranova, and A.V. Titov for discussion and MEXT, INTAS 001-0233, and QUB/IRCEP for support.

*Also at Moscow Institute of Physics and Technology, Russia.
Electronic address: http://wwwapr.apr.jaeri.go.jp/aprc/e/results/simulation/timur/piston/
†Also at General Physics Institute of RAS, Russia.

[1] T. Zh. Esirkepov *et al.*, JETP Lett. **70**, 82 (1999); S.V. Bulanov *et al.*, Plasma Phys. Rep. **25**, 701 (1999); S.V. Bulanov *et al.*, JETP Lett. **71**, 407 (2000); K. Nishihara *et al.*, Nucl. Instrum. Methods Phys. Res., Sect. A **464**, 98 (2001).
[2] A.V. Gurevich *et al.*, Sov. Phys. JETP **22**, 449 (1966).
[3] T. Ditmire *et al.*, Phys. Rev. A **53**, 3379 (1996).
[4] G. S. Sarkisov *et al.*, Phys. Rev. E **59**, 7042 (1999).
[5] A.V. Kuznetsov *et al.*, Plasma Phys. Rep. **27**, 211 (2001).
[6] T. Tajima and G. Mourou, Phys. Rev. ST Accel. Beams **5**, 031301 (2002); I. N. Ross *et al.*, Opt. Commun. **144**, 125 (1997).
[7] A. D. Steiger and C. H. Woods, Phys. Rev. A **5**, 1467 (1972); Ya. B. Zel'dovich and A. F. Illarionov, Sov. Phys. JETP **34**, 467 (1972); A. Zhidkov *et al.*, Phys. Rev. Lett. **88**, 185002 (2002); S.V. Bulanov, T. Zh. Esirkepov, J. Koga, and T. Tajima, Plasma Phys. Rep. **30**, 196 (2004).
[8] V. I. Veksler, in *Proceedings of CERN Symposium on High Energy Accelerators and Pion Physics, Geneva, 1956* (European Organization for Nuclear Research, Geneva, 1956), Vol. 1, p. 80; At. Energy **2**, 427 (1957).
[9] M. Ashour-Abdalla *et al.*, Phys. Rev. A **23**, 1906 (1981).
[10] G. A. Askar'yan, At. Energy **4**, 71 (1958).
[11] E. M. Lifshitz, J. Phys. USSR **10**, 116 (1946); S. Weinberg, *Gravitation and Cosmology* (John Wiley and Sons, Inc., New York, 1972).
[12] T. Zh. Esirkepov, Comput. Phys. Commun. **135**, 144 (2001).
[13] S.V. Bulanov *et al.*, in *Reviews of Plasma Physics*, edited by V. D. Shafranov (Kluwer Academic/Plenum Publishers, New York, 2001), Vol. 22, p. 227.
[14] L. D. Landau and E. M. Lifshitz, *The Classical Theory of Fields* (Pergamon Press, Oxford, 1980); W. Pauli, *Theory of Relativity* (Dover, New York, 1981).
[15] F.V. Hartemann, *High-Field Electrodynamics* (CRC Press, New York, 2002).
[16] T. Ludlam and L. McLerran, Phys. Today **56**, No. 10, 48 (2003).